FLAW GEOMETRY RECONSTRUCTION USING A LIMITED SET OF X-RAY RADIOGRAPHIC PROJECTIONS

Richard M. Wallingford and John P. Basart

Department of Electrical and Computer Engineering
Center for Nondestructive Evaluation
Iowa State University
Ames, IA 50011

INTRODUCTION

Flaw detection using x-ray radiography has traditionally been based on a qualitative assessment of the x-ray image features [1]. This approach, although reliable in many cases, has limitations due to the relatively small amount of information contained in a single projected image, the variability of inspection results based on the radiographer's experience level and intuition, and the inability to extract quantitative information about the flaw. One way to help alleviate these limitations is to use x-ray computed tomography (CT) where the flaw can be reconstructed, sized, and located within the part [2,3,4,5]. The drawback of using CT is that the hardware required is very complex and expensive. In addition, the computational power required to execute a CT algorithm in a reasonable amount of time is very high [6,7]. A compromise between the use of a single x-ray projection and CT for flaw reconstruction is to model the flaw, a priori, as a geometric figure or solid and reconstruct the model from a reduced set of x-ray projections [8]. The number of projections required to deduce the geometric model parameters may vary with the complexity of the model, but it will be shown that only two projections are required to reconstruct a straight line of arbitrary orientation. In this paper we present the reconstruction formulation for a crack modeled as a straight line or series of straight lines. We also present the analysis for reconstruction errors caused by film measurement errors and system geometry errors. Experimental results of flaw reconstruction with a microfocus x-ray machine are also presented.

MODELING AND RECONSTRUCTION OF CRACK-LIKE FLAWS

One possible model for a crack-like flaw is an arbitrarily oriented straight line or a piecewise linear connection of such lines. This simple model, represents an attractive starting point for model development since reconstruction of other, more complicated, models will use the same ideas. The reconstruction of an arbitrarily oriented straight line essentially involves the reconstruction of two points in space, namely the endpoints of the line. The location of these endpoints can be computed from two projections of the sample. A key element to this work is the method in which the two projections are obtained. One criterion for the method is that it must be easily implemented using standard microfocus x-ray equipment. To meet this criterion, the two projections are made by moving the sample a known distance in a direction perpendicular to the source-film axis as shown in Fig. 1. This is most easily accomplished by placing the sample on a motorized x-y stage and by moving the stage to produce a new projection. The crack model can be reconstructed from two projections assuming a cone beam generated by a microfocus x-ray source. A non microfocus source cannot be used with this method because of the geometric unsharpness created when the sample is in the magnification regime.

DERIVATION OF RECONSTRUCTION EQUATIONS

The equations for reconstructing the crack endpoints are derived by considering the diagram shown in Fig. 2. A straight crack with endpoints (x_{c1}, y_{c1}, z_{c1}) and (x_{c2}, y_{c2}, z_{c2}) within a sample is illustrated with its projection onto the x-ray film. The crack projection is defined by the line connecting the film points (x_{11}, y_{11}) and (x_{12}, y_{12}). Also shown is the sample, translated by an amount Δx, and the new crack projection defined by the line connecting the film points (x_{21}, y_{21}) and (x_{22}, y_{22}). The four rays passing from the x-ray source to the film through the four crack endpoints can be described by a parameterized equation of the form

$$\vec{V} = \vec{V}_f + t\left(\vec{V}_s - \vec{V}_f\right) \tag{1}$$

where

$\vec{V}_f$ = vector from the origin to the intersection of the ray with the film

$$= x_{pq}\,\hat{i} + y_{pq}\,\hat{j} \qquad p,q = 1,2 \tag{2}$$

$\vec{V}_s$ = vector from the origin to the x–ray source

$$= x_s\,\hat{i} + y_s\,\hat{j} + z_s\,\hat{k} \tag{3}$$

($\hat{i}, \hat{j}, \hat{k}$ are unit vectors in the x, y, and z directions, respectively.)

and $0 < t < 1$.

The vector, $\vec{V}$, initiates at the origin and, depending upon the value of the parameter, t, terminates at some point along the ray between the film and the source. Thus, at some value, t_c, $\vec{V}$ must terminate on the crack endpoint. The goal is to determine the four parameters t_1, t_2, t_3, and t_4 of the four vector equations describing the rays such that the four vectors terminate on the crack endpoints represented by c subscripts. The coordinates of the endpoints can then be computed. Using the coordinate system in Fig. 2, the four vector equations are

$$\vec{V}_1 = x_{11}\hat{i} + y_{11}\hat{j} + t_1\left\{(x_s - x_{11})\hat{i} + (y_s - y_{11})\,\hat{j} + z_s\hat{k}\right\} \tag{4}$$

$$\vec{V}_2 = x_{12}\hat{i} + y_{12}\hat{j} + t_2\left\{(x_s - x_{12})\hat{i} + (y_s - y_{12})\,\hat{j} + z_s\hat{k}\right\} \tag{5}$$

$$\vec{V}_3 = x_{21}\hat{i} + y_{21}\hat{j} + t_3\left\{(x_s - x_{21})\hat{i} + (y_s - y_{21})\,\hat{j} + z_s\hat{k}\right\} \tag{6}$$

$$\vec{V}_4 = x_{22}\hat{i} + y_{22}\hat{j} + t_4\left\{(x_s - x_{22})\hat{i} + (y_s - y_{22})\,\hat{j} + z_s\hat{k}\right\} \tag{7}$$

By constraining the vectors to terminate on the crack endpoints and assuming that the crack translation is in the x-direction only, we can write the following equations:

$$\vec{V}_1 = x_{c1}\hat{i} + y_{c1}\hat{j} + z_{c1}\hat{k} \tag{8}$$

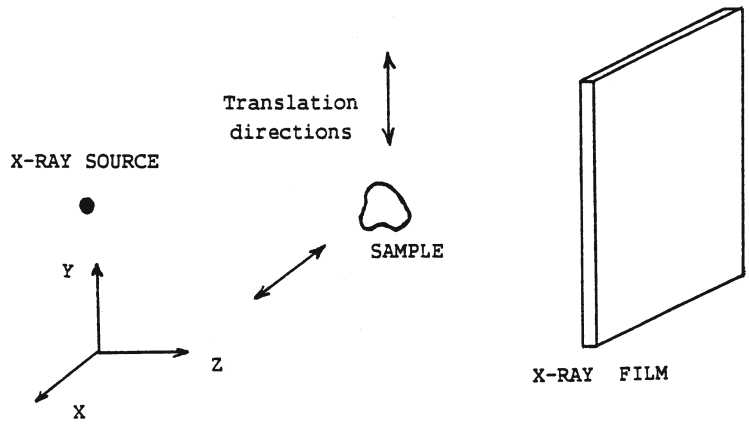

Fig. 1. Illustration of Geometry used with the projection method.

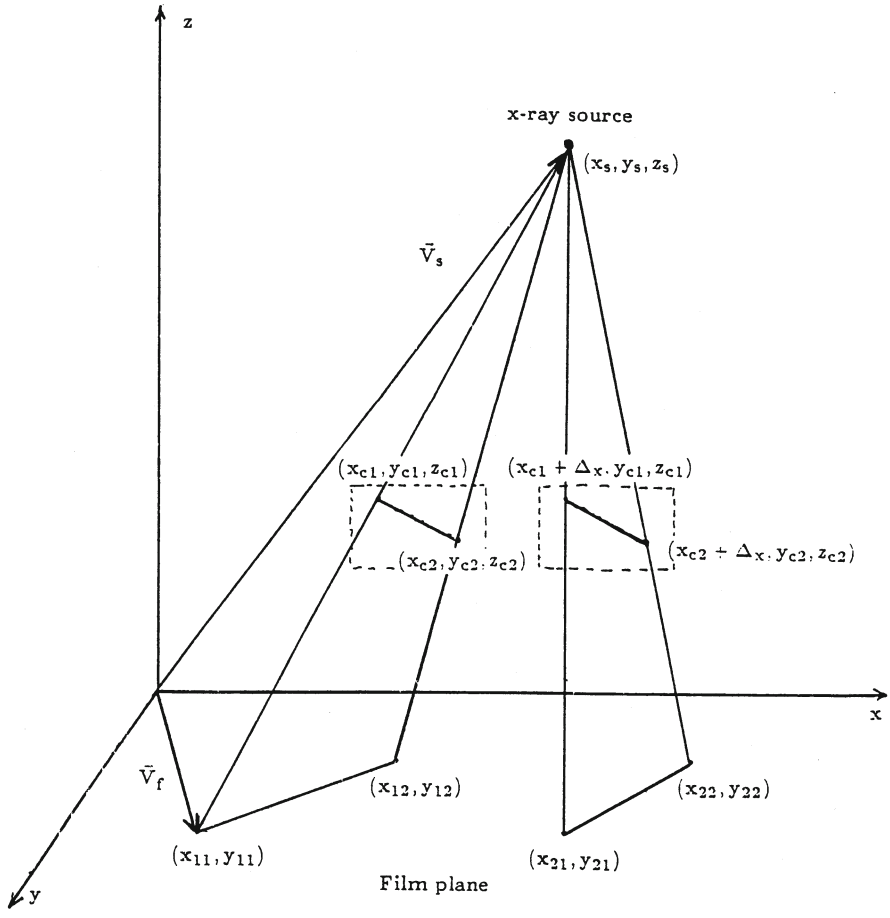

Fig. 2. Two projections of a crack-like flaw.

$$\vec{V}_2 = x_{c2}\hat{i} + y_{c2}\hat{j} + z_{c2}\hat{k} \tag{9}$$

$$\vec{V}_3 = \left(x_{c1} + \Delta x\right)\hat{i} + y_{c1}\hat{j} + z_{c1}\hat{k} \tag{10}$$

$$\vec{V}_4 = \left(x_{c2} + \Delta x\right)\hat{i} + y_{c2}\hat{j} + z_{c2}\hat{k} \tag{11}$$

Notice that $\vec{V}_1$ and $\vec{V}_2$ in Eqs. (8) and (9) are vectors from the origin to the untranslated crack endpoints, and that $\vec{V}_3$ and $\vec{V}_4$ in Eqs. (10) and (11) are vectors from the origin to the translated crack endpoints. Equating the $\hat{i}$ components and the $\hat{k}$ components of Eqs. (8)-(11) with (4)-(7) respectively allows us to write the following:

$$t_1 z_s = z_{c1} \tag{12}$$

$$t_2 z_s = z_{c2} \tag{13}$$

$$t_3 = t_1 \tag{14}$$

$$t_4 = t_2 \tag{15}$$

$$x_{c1} = x_{11} + t_1\left(x_s - x_{11}\right) \tag{16}$$

$$x_{c1} + \Delta x = x_{21} + t_1\left(x_s - x_{21}\right) \tag{17}$$

$$x_{c2} = x_{12} + t_2\left(x_s - x_{12}\right) \tag{18}$$

$$x_{c2} + \Delta x = x_{22} + t_2\left(x_s - x_{22}\right) \tag{19}$$

Subtracting Eq. (16) from (17), and Eq. (18) from (19), expressions for the parameters t_1 and t_2 can be written as:

$$t_1 = \frac{\left(x_{11} - x_{21} + \Delta x\right)}{\left(x_{11} - x_{21}\right)} \tag{20}$$

$$t_2 = \frac{\left(x_{12} - x_{22} + \Delta x\right)}{\left(x_{12} - x_{22}\right)} \tag{21}$$

The crack coordinates x_{c1}, x_{c2}, z_{c1}, and z_{c2} can now be determined by substituting the above expressions for t_1 and t_2 in Eqs. (12),(13),(16) and (18). The y-coordinates of the crack endpoints, y_{c1} and y_{c2}, are computed by equating the $\hat{j}$ components of Eqs. (8) and (9) with (4) and (5) respectively, and are given by Eqs. (22) and (23).

$$y_{c1} = y_{11} + t_1 \left(y_s - y_{11} \right) \tag{22}$$

$$y_{c2} = y_{12} + t_2 \left(y_s - y_{12} \right) \tag{23}$$

In the case where the crack is best modeled as a series of connected straight lines, each straight line is considered as a separate reconstruction problem. Corresponding straight lines of a piecewise linear model must be identified in the two projections followed by reconstruction of the straight line endpoints using the method described previously. The reconstruction procedure is then repeated for each straight segment of the model. Care must be taken to correctly and accurately identify corresponding endpoints in the two projections of a straight segment in the model. If the crack takes a sharp turn or bend, this point can be identified quite accurately, however, if the crack changes directions slowly as in a curve, the best approach is to select the midpoint between two accurately identifiable points [9]. This results in accurate point correspondence between the two projections since the midpoints of the projections of any curved segment correspond to the same point on the curved projector.

RECONSTRUCTION ERROR ANALYSIS

In order to understand effects of measurement errors on the crack reconstruction error, expressions have been derived which relate the reconstruction error to the various uncertainties associated with film coordinate measurements and source coordinate measurements. By writing the crack coordinates in terms of the various measured coordinates, an error bound can be derived by taking the total differential of the equation. For example, the crack coordinate x_{c1} can be written as a function of the following form:

$$x_{c1} = f_{x_{c1}} \left(x_{11}, x_{21}, x_s; \Delta x \right) \tag{24}$$

The total differential of this function is thus,

$$dx_{c1} = \frac{\partial f_{x_{c1}}}{\partial x_{11}} dx_{c1} + \frac{\partial f_{x_{c1}}}{\partial x_{21}} dx_{21} + \frac{\partial f_{x_{c1}}}{\partial x_s} dx_s \tag{25}$$

An approximate expression for the reconstruction error can now be written as:

$$\Delta x_{c1} \cong \frac{\partial f_{x_{c1}}}{\partial x_{11}} \Delta x_{11} + \frac{\partial f_{x_{c1}}}{\partial x_{21}} \Delta x_{21} + \frac{\partial f_{x_{c1}}}{\partial x_s} \Delta x_s \tag{26}$$

Equation (26) allows us to compute the error in x_{c1} due to estimated uncertainties in the measured quantities x_{11}, x_{21}, and x_s. If upper bounds in the measurement uncertainties are used, the resulting reconstruction error will also be an upper bound. In the case where multiple measurements of each parameter are made, the variance of the reconstructed coordinate can be used as an error measure. The equation for the x_{c1}-coordinate variance is given by the standard propagation of error formula,

$$\sigma^2_{x_{c1}} = \left(\frac{\partial f_{x_{c1}}}{\partial x_{11}} \right)^2 \sigma^2_{x_{11}} + \left(\frac{\partial f_{x_{c1}}}{\partial x_{21}} \right)^2 \sigma^2_{x_{21}} + \left(\frac{\partial f x_{c1}}{\partial x_s} \right)^2 \sigma^2_{x_s} \tag{27}$$

Error equations for the other crack coordinates can be derived in a similar fashion. The study of these equations is useful in determining how the various parameters influence the error. In particular, it is helpful to know which source-sample-film geometries and which sample translation distances can help minimize the reconstruction error. For example, source coordinate errors dominate the absolute reconstruction error when a large magnification is

used, while film coordinate measurement errors dominate at low magnifications. Thus, when source measurement errors are known to be large, the reconstruction error can be minimized by performing the radiography under low magnification. Film coordinate measurement errors are caused by uncertainty in the distance measurements from the coordinate origin to the projected crack endpoints as well as image unsharpness, but are usually small because the uncertainty is quite low and the microfocus source produces a sharp image.

EXPERIMENTAL RESULTS

The crack reconstruction method was tested experimentally by taking two projections of a needle stuck into a paraffin slab with a microfocus x-ray machine. A diagram showing the experimental setup is shown in Fig. 3. A reference projection of the paraffin-needle sample was first produced on a single sheet of DEF-5 X-ray film. A second radiograph on a different sheet of film was produced by translating the sample with a movable x-y stage. An absolute coordinate system was established for measuring the film and source coordinates by shadowing a fixed pinhead onto both films. The shadow of the pinhead was used as the coordinate origin in both radiographs. The film coordinates as well as the x-ray source coordinates were measured with respect this point.

The following parameters were measured:

(x_s, y_s, z_s)	= (85, 9, 572) mm
(x_{11}, y_{11})	= (144.0, 20.0) mm
(x_{12}, y_{12})	= (114.0, -50.0) mm
(x_{21}, y_{21})	= (38.0, 20.0) mm
(x_{22}, y_{22})	= (2.0, -50.0) mm
$(\Delta x, \Delta y)$	= (-51.0, 0.0) mm
needle length	= 41 mm
z_{c1}	= 283 mm

The uncertainty on each film coordinate measurement is 0.5 mm and the uncertainty in the source coordinate measurements is 2 mm. The sample translation distance, Δx, is assumed to be error free. Applying reconstruction equations (16),(18),(22) and (23), the following quantities were computed:

(x_{c1}, y_{c1}, z_{c1})	= (113, 14, 297) mm
(x_{c2}, y_{c2}, z_{c2})	= (98, -18, 312) mm
needle length	= 38.5 mm

The following error bars were computed for the reconstructed crack coordinates and the needle length.

Δx_{c1}	= 1.3 mm
Δx_{c2}	= 1.3 mm
Δy_{c1}	= 1.3 mm
Δy_{c2}	= 1.6 mm
Δz_{c1}	= 3.6 mm
Δz_{c2}	= 3.4 mm
needle length	= 6.1 mm

The agreement between the estimated and measured values for the needle length is within 6% and the reconstructed needle length is well within the computed error bar. Although the results of this experiment produce only one sample point for comparison, we are encouraged

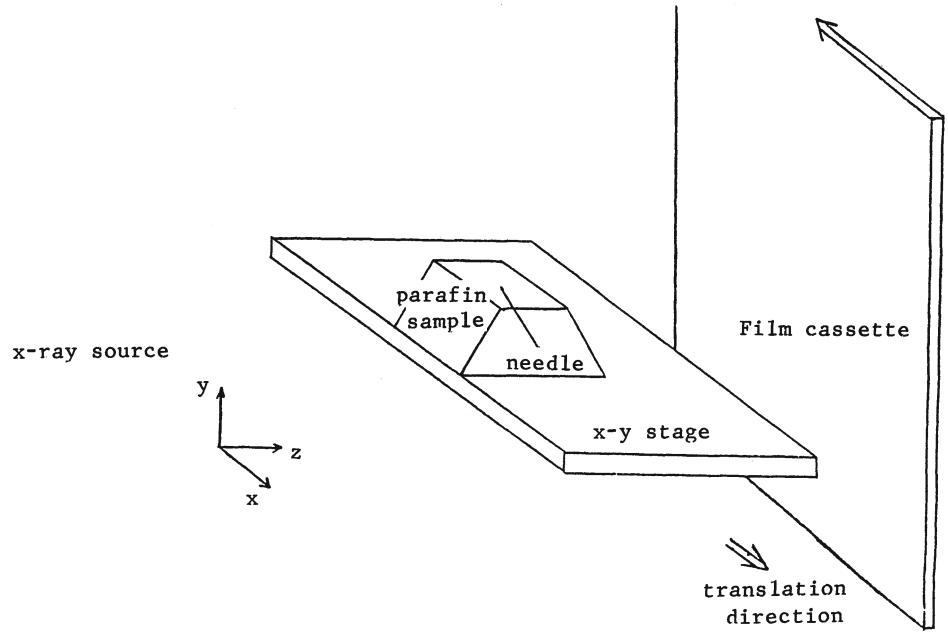

Fig. 3. Experimental configuration.

by them. Multiple experiments will be performed for a complete error analysis in the future. Future work will also be done in designing measurement techniques which minimize the error bars.

CONCLUSION

A method for reconstructing cracks modeled as straight lines or a series of straight lines using two radiographic projections has been derived. Experimental results using this method are very encouraging and it appears that this may be a good method for sizing and locating cracks. The next step of this work is to extend this technique to volumetric flaws with geometric solid models. As long as unique points in the projected radiographs can be identified, these points can be reconstructed in 3-D using the technique described here. In addition, model validity issues are being investigated as well as the automation of this technique using digital radiography.

ACKNOWLEDGMENT

The authors thank Joe Gray for his useful advice and for the use of his X-Ray equipment. This work was supported by the Center for NDE at Iowa State University.

REFERENCES

1 Industrial Radiology - Theory and Practice. R. Halmshaw, Applied Science Publishers, New Jersey, 1982.

2 The Radon Transform and Some of its Applications. Stanley R. Deans, John Wiley, New York, 1983.

3. R. L. Hack. D K. Archipley-Smith, and W. H. Pfeifer, in Review of Progress in Quantitative NDE, edited by D. O. Thompson and D. E. Chimenti, (Plenum Press, New York, 1987), Vol. 6A, pp. 401-410.

4 M. W. Vannier and W. A. Ellingson, in Review of Progress in Quantitative NDE, Press, New York, 1988), Vol. 7A, pp. 373-380.

5 R. S. Ledley, "Introduction to Computerized Tomography,", in Comput. Biol. Med., Vol. 6, pp.239-246.

6 Selected Topics in Image Science, Vol. 23 Lecture Notes in Medical Informatics. Edited by O. Nalcioglu and Z. H. Cho. Springer-Verlag, New York, 1984.

7 Hui Peng and Henry Stark, "Direct Fourier Reconstruction in Fan-Beam Tomography," in IEEE Transactions on Medical Imaging, Vol. MI-6, No. 3 September, 1987.

8 J. N. Gray and B. Shull, "Three Dimensional Modeling of Projection X-Ray Radiography," to be published in Review of Progress in Quantitative NDE, (Plenum Press, New York, 1989), Vol. 8.

9 J. K. Aggarwal, L. S. Davis and W. N. Martin, "Correspondence Processes in Dynamic Scene Analysis," in Proceedings of the IEEE, Vol. 69, No. 5, pp. 562-572, (1981).